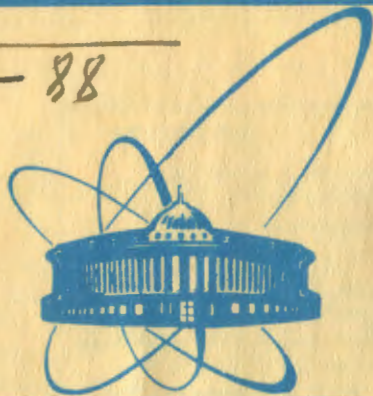


Z-88



сообщения  
объединенного  
института  
ядерных  
исследований  
дубна

7

2406/2-81

18/5-81

E11-81-88

G.Zschornack, G.Müller, G.Musiol

GEOMC – A MONTE-CARLO PROGRAM  
FOR CALCULATING GEOMETRICAL  
ABERRATIONS  
IN CURVED-CRYSTAL SPECTROMETERS

1981

## 1. INTRODUCTION

In recent years the technical and methodical progress on several technical fields and physics understanding has contributed to an increase in the accuracy of curved-crystal diffraction spectrometers and has excluded a series of aberrations typical for spectrometer operation. Essentially, most of aberrations which might occur with a curved-crystal spectrometer can be negligible by a careful construction, alignment and operation of the spectrometer. However, it should be known the types of aberrations which can occur and their relative magnitudes. Some aberrations produce a line shift, others contribute only to broadening the line. Line shifts could affect in systematic errors in measurements of the wavelengths or energies. Especially, this problem takes a leading part at the absolute determination of the wavelengths or energies.

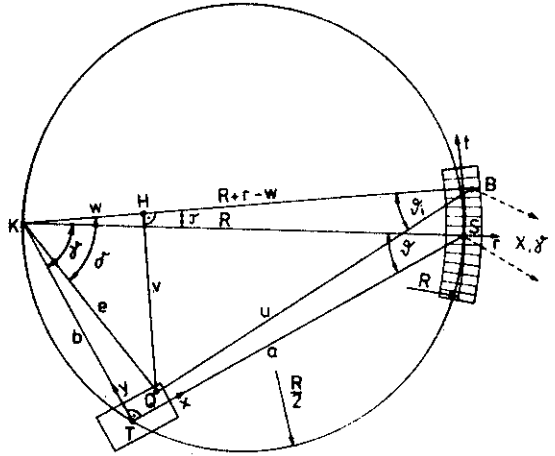
In this paper we describe a Monte-Carlo program GEOMC to investigate centroid shifts and shape alterations of the diffraction line due to the finite size of source and crystal, i.e., the effect of geometrical aberrations for the Laue and for the Bragg case. This problem was approached for transmission spectrometers (Laue case) by Schwitz et al.<sup>1/</sup> and also, it was taken into consideration by Schult<sup>2/</sup> and Reidy<sup>3/</sup>. For the Bragg case, this problem was discussed, for instance, by Meisel et al.<sup>4/</sup> and Zschornack et al.<sup>5/</sup>. The present program doesn't take into consideration crystal structure effects, radiation absorption and extinction, and the effects, originated in errors of the crystal bending.

## 2. THE MATHEMATICAL TREATMENT

### 2.1. The Laue Case

For transmission geometry the mathematical treatment was worked out by Schwitz et al.<sup>1/</sup>. The geometry of the problem is shown schematically in projection in fig.1. The coordinates of an arbitrary emission point  $Q(x,y,z)$  of the source are defined from the point  $T$  at the focal circle; and these coordinates of any diffraction point  $B(r,t,h)$  of the crystal, from the point  $S$  of the same circle. The latter point lies opposite to the intersection  $K$  of the axis of curvature,  $z$  and  $h$

Fig.1. Schematic geometry of a curved Laue crystal spectrometer in Du Mond version. T - source reference point on the focal circle; Q - projection of an arbitrary source point (coordinates  $x, y, z$ ) on the drawing plane; K - intersection of the axis of curvature with the drawing plane; S - crystal reference point on the focal circle; B - projection of an arbitrary diffraction point (coordinates  $r, t, h$ ) on the drawing plane;  $\theta$  - measured spectrometer angle between the direction of a photon emitted in T and diffracted in S and the crystal plane through S;  $\theta_i$  - projection of the effective diffraction angle of a photon emitted in Q and diffracted in B; R - crystal radius of curvature.



are perpendicular to the plane, which contain the focal circle. The angle between the ray from T to S and the crystal plane through S is denoted as  $\theta$ . The angle between the line joining the arbitrary points Q and B and the crystal through B is denoted as  $\theta_i$ . From the geometry in fig.1 we derive the quantities

$$a = R \cos \theta, \quad (1)$$

$$b = R \sin \theta, \quad (2)$$

$$v = e \sin \delta, \quad (3)$$

$$w = e \cos \delta, \quad (4)$$

$$r = t/R, \quad (5)$$

$$\sin \delta = \frac{1}{e} [(b-y) \cos(\theta-r) - x \sin(\theta-r)], \quad (6)$$

$$\cos \delta = \frac{1}{e} [(b-y) \sin(\theta-r) + x \cos(\theta-r)]. \quad (7)$$

The insertion of eqs. (6) and (7) in eqs. (3) and (4) yields:

$$v = (b-y) \cos(\theta-r) - x \sin(\theta-r), \quad (8)$$

$$w = (b-y) \sin(\theta-r) + x \cos(\theta-r). \quad (9)$$

The segment length  $u$  can be expressed as:

$$u^2 = (R+r-w)^2 + v^2 + (h-z)^2 \quad (10)$$

To take into consideration the triangle QBH,  $\sin \theta_i$  has the form

$$\sin \theta_i = \frac{v}{u} = \frac{v}{[(R+r-w)^2 + v^2 + (h-z)^2]^{1/2}} \quad (11)$$

Due to the crystal curvature, the lattice spacing changes across the plate as a function of the coordinates  $r$ :

$$d_i = (1 + \frac{r}{R}) d, \quad (12)$$

where  $d$  is the unstrained crystal interplanar spacing distance. The Bragg law valid for each individual ray can be written:

$$2 d_i \sin \theta_i = 2 d (1 + \frac{r}{R}) \sin \theta_i = m \lambda, \quad (13)$$

where  $\lambda$  is the wavelength of the diffracted ray and  $m$  is the order of diffraction. Thus, we define the quantity:

$$(\sin \theta_i)_{\text{eff}} = (1 + \frac{r}{R}) \sin \theta_i = \frac{(1 + \frac{r}{R}) \cdot \frac{v}{R}}{[(1 + \frac{r}{R} - \frac{w}{R})^2 + (\frac{v}{R})^2 + (\frac{h-z}{R})^2]^{1/2}} \quad (14)$$

We use formula (14) as a starting point for the treatment of the Laue case in the Monte-Carlo program.

## 2.2. The Bragg Case

For the reflection case the mathematical treatment was worked out by Schwitz et al.<sup>/1/</sup>. The geometry of the problem is shown as the analogous one to the Laue case in fig.2.

By analogy with this, we derive the quantities

$$a = R \sin \theta, \quad (15)$$

$$b = R \cos \theta. \quad (16)$$

We note, that the quantity  $R'$  in fig.2 is equal to  $R$  for the description of Johann<sup>/6/</sup> spectrometers, but has the form  $R \cos \theta$  for Johansson<sup>/7/</sup> spectrometers.

The eqs. (3), (4) and (5) don't change their forms, so that we get



The used strategy is based on the same principle as applied by Schwitz et al.<sup>1/</sup>. We specify the diffraction pattern  $f(\theta_i)$  by a Gaussian function:

$$f(\theta_i) = \exp \left[ - \frac{(\theta_i - \theta_B)^2}{2\sigma^2} \right], \quad (21)$$

where  $\theta_B$  denotes the Bragg angle corresponding to the wavelength of the incident photon,  $\sigma$  is a free parameter depending on the mosaic spread in the crystal. Further on, we assume that the radiation is strongly monochromatic and that the spectrometer setting angle  $\theta$  is closed to the corresponding Bragg angle  $\theta_B$ . The observed reflex is given by

$$F(\theta) = \frac{1}{v} \int_v \exp \left[ - \frac{(\theta_i(\theta, \vec{x}) - \theta_B)^2}{2\sigma^2} \right] dv \quad (22)$$

with  $\theta_i$  = effective diffraction angle and  $\theta_i(\theta, \vec{x}) = \theta_i(\theta, x, y, z, r, t, h) = \theta_i$ ,  $v$  = 6-dimensional source-crystal volume.

To obtain the value of the integral (22) for any geometrical condition we define a distribution function  $D(\hat{\theta} - \theta)$  as Schwitz et al.<sup>1/</sup> and Schult<sup>2/</sup> did independently of the diffraction pattern.

$$D(\hat{\theta} - \theta) = \frac{1}{v} \int_v \delta[\sin(\theta, \vec{x}) - \sin \hat{\theta}] dv, \quad (23)$$

where  $\delta$  is the Dirac  $\delta$ -function and  $\hat{\theta}$  is an arbitrary effective diffraction angle. To understand the significance of  $D$ , we note that  $v \cdot D(\hat{\theta} - \theta) d\hat{\theta}$  represents the part of the 6-dimensional source-crystal volume for which the effective diffraction angle ranges between  $\hat{\theta}$  and  $\hat{\theta} + d\hat{\theta}$ . Then we have:

$$F(\theta) = \int_{\hat{\theta}} D(\hat{\theta} - \theta) f(\hat{\theta}) d\hat{\theta}. \quad (24)$$

### 3. THE PROGRAM GEOMC

To obtain practical results, we have developed the program GEOMC, which calculates the problem by the Monte-Carlo method.

#### 3.1. The Main Program GEOMC

The main program prepares all the data for the following data processing. The data input stream has the form (data cards):

1. A(I) (10A8)  
A(I) - heading text to characterize the problem
2. NTYP1, NTYP2 (215)  
NTYP1 - selection of the diffraction case

- =1 for the Bragg case
- =2 for the Laue case
- NTYP2 - characterize the type of the curved Bragg spectrometer
  - =1 for a Johann spectrometer
  - =2 for a Johansson spectrometer
- 3. N, NSPEK, NW, EMASMC, EMASD (3I10, 2F10.0)
  - N - number of events at one meshpoint for integrating eqs. (20) or (14) to get the average value of  $\sin\theta_i$
  - NSPEK - number of meshpoints for the integration of eqs. (20) or (14)
  - NW - number of meshpoints for the generation of the distribution function  $D(\hat{\theta}-\theta)$
  - EMASMC - step width between the single meshpoints in the integration of eqs. (20) or (14) in arcsec
  - EMASD - step width between the meshpoints at the construction of the distribution function  $D(\hat{\theta}-\theta)$  in arcsec.
- 4. R, SIG1, TB1, TSTEU (4 F 10.0)
  - R - Diameter of the Rowland circle in mm
  - SIG1 - Variance, depending on the mosaic spread in the crystal in arcsec
  - TB1 - Bragg diffraction angle in degrees
  - TSTEU - Control parameter. If TSTEU set to 0, no integration of eqs. (20) or (14) occurs. Only the distribution function  $D(\hat{\theta}-\theta)$  is generated. If TSTEU is not equal to 0, both the integration of eqs. (20) or (14) are performed and the distribution  $D(\hat{\theta}-\theta)$  is calculated.
- 5. X1, X2, Y1, Y2, Z1, Z2 (6 F 10.0)
  - X1, X2 - coordinates of the source depth limits in mm
  - Y1, Y2 - coordinates of the source width limits in mm
  - Z1, Z2 - coordinates of the source height limits in mm
- 6. R1, R2, T1, T2, H1, H2 (6 F 10.0)
  - R1, R2 - coordinates of the crystal depth limits in mm
  - T1, T2 - coordinates of the crystal width limits in mm
  - H1, H2 - coordinates of the crystal height limits in mm

To start a new calculation, one must repeat the new input data in form of the cards 1 to 6. To end the calculations,

one have to add three blank cards. In the common block CR the array X is used to store the results of the calculated reflex or the distribution function  $D(\hat{\theta}-\theta)$ . In CR the parameters EMASMC, EMASD, SIG1, NTYP1 and NTYP2 are already specified above. The array F(I) contains a Gaussian shaped standard peak with the variance  $\sigma$  for the determination of the reflex profile by the convolution with the function  $D(\hat{\theta}-\theta)$ .

The printed output contains all the information about the input data and characterizes the geometry in which the calculations are performed. If TSTEU is not equal to 0, the reflex profile generated from subroutine MONT 1 is printed. After these results the distribution function  $D(\hat{\theta}-\theta)$  and the result of the convolution from  $D(\hat{\theta}-\theta)$  with a Gaussian shaped peak is plotted. After the output of the reflex profile from MONT 1, the distribution function and the reflex profile from the convolution procedure are printed out. Each time the peak shifts,  $\sigma$  and corresponding full width at half maximum of a symmetric Gaussian peak are plotted.

### 3.2. The Subprogram MONT 1

The subroutine MONT 1 (RR, SIGM, X1, XD, Y1, YD, Z1, ZD, R1, RD, T1, TD, H1, HD, TB, TK, N, NSPEK) is written to calculate the reflex profile  $F(\theta_i)$ . Thereby,  $\sin \theta_i$  is calculated from formula (14) for the Laue case and from formula (20) for the Bragg case.

The parameter list contains the following new notations:

- RR - diameter of the Rowland circle
- SIGM - two times of  $\sigma^2$  in arcsec
- TK - conversion factor for the conversion degrees to arcsec ( $TK = \pi/6.48 \cdot 10^5$ )

The quantities

$$\begin{array}{ll} XD = X2 - X1 & RD = R2 - R1 \\ YD = Y2 - Y1 & TD = T2 - T1 \\ ZD = Z2 - Z1 & HD = H2 - H1 \end{array} \quad (25)$$

denote the integration interval for the 6-dimensional volume. To generate random coordinates for the integration of eqs. (14) or (20), we use the generator RANF to generate equipartitioned random numbers. For instance, the random coordinate x we construct by

$$x = X1 + XD \cdot \text{RANF} \quad (26)$$

All the other coordinates we construct by analogy with formula (26).

### 3.3. The Subprogram WEIGHT

The subroutine WEIGHT (PI, TB, X1, XD, Y1, YD, Z1, ZD, R1, RD, T1, TD, H1, HD, RR, N1) generates the distribution function  $D(\hat{\theta}-\theta)$  after formula (23). The generation of random coordinates and the computation of  $\sin\theta_i$  occurs by analogy to the procedure used in MONT 1. N1 is mapped to the quantity NW. The calculation results are stored in the array X(I).

### 3.4. The Subprogram FALT

The subroutine FALT (A, B, C, S1, N) provides the convolution of a Gaussian shaped standard peak with the distribution function  $D(\hat{\theta}-\theta)$ . The parameter list includes the following notations:

- A - Distribution function  $D(\hat{\theta}-\theta)$ .
- B - Gaussian shaped standard peak.
- C - Result of the convolution, e.g., the profile of the diffracted line.
- S1 - The peak area of the diffraction profile.
- N - Field length for the convolution procedure.

We note that the results from the subroutine MONT1 are the same as from WEIGHT with following convolution with a Gaussian shaped standard peak. Using the subprogram MONT1, one can fix the statistics for each meshpoint, but on using WEIGHT one can determine the integral number of events under the diffraction profile.

To get a sufficient accuracy, one must take into account, that the error  $\bar{\sigma}_I$  of the Monte-Carlo-integration falls only as the following one

$$\bar{\sigma}_I \approx N^{-1/2}, \quad (27)$$

where N is the number of the calculated function values.

### 3.5. The Subprogram VERT

The subroutine VERT (ZE, S1, S2, S3, K, L) serves only, for a first view, to value the obtained results. In the array ZE the diffraction profile is stored and S1, S2 and S3 denote the peak area, peak shift and the standard variance  $\sigma$ , respectively. For asymmetric problems the computation of  $\sigma$  is not accurate and it is recommendable to use a more perfect processing routine. In our case the reflex processing occurs by using the moment method.

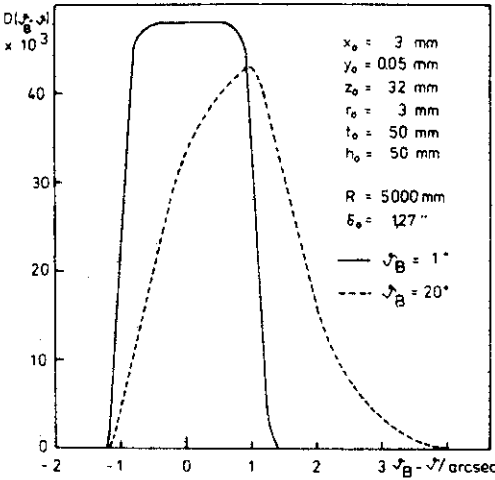
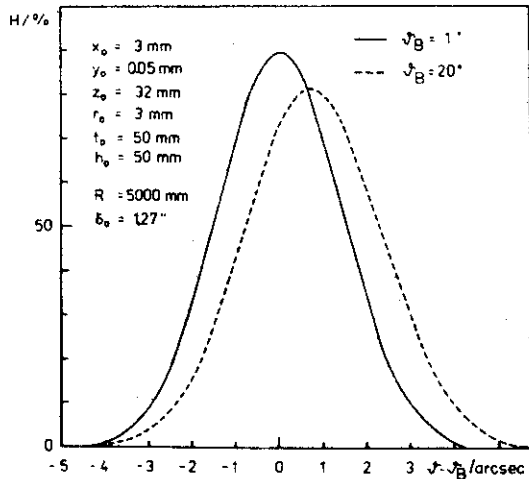


Fig.3. Distribution function  $D(\theta_B - \theta)$  in arbitrary units for the Laue case.

Fig.4. Reflex profile, following after the convolution from Gaussian shaped diffraction pattern (maximum amplitude 1) with the distribution functions  $D(\theta_B - \theta)$  as shown in Fig.3. The reflex amplitude (in percent) is related to the maximum amplitude of the diffraction pattern.



#### 4. NUMERICAL EXAMPLES

For demonstration we have carried out calculations for two concrete geometries in the Bragg and Laue case. For the Laue case we have assumed a geometry, typically for the Du Mont spectrometer from the University of Fribourg<sup>8/</sup>.

$$\begin{array}{lll}
 x_0 = 3 \text{ mm} & r_0 = 3 \text{ mm} & R = 5000 \text{ mm} \\
 y_0 = 0.05 \text{ mm} & t_0 = 50 \text{ mm} & \sigma = 1.27^\circ \\
 z_0 = 32 \text{ mm} & h_0 = 50 \text{ mm} &
 \end{array}$$

For the Bragg case we assume

$$\begin{array}{lll} x_0 = 3 \text{ mm} & r_0 = 0 \text{ mm} & R = 648 \text{ mm} \\ y_0 = 0.1 \text{ mm} & t_0 = 40 \text{ mm} & \sigma = 5'' \\ z_0 = 10 \text{ mm} & h_0 = 10 \text{ mm} & \end{array}$$

In both cases a symmetric position of crystal and source is suggested.

Figure 3 shows the calculated distribution function  $D(\hat{\theta}-\theta)$  and fig.4 computed reflex profiles for the Laue case, using the values given above. Figures 5 and 6 show the reflex profiles for the Bragg case in Johann and Johansson geometry.

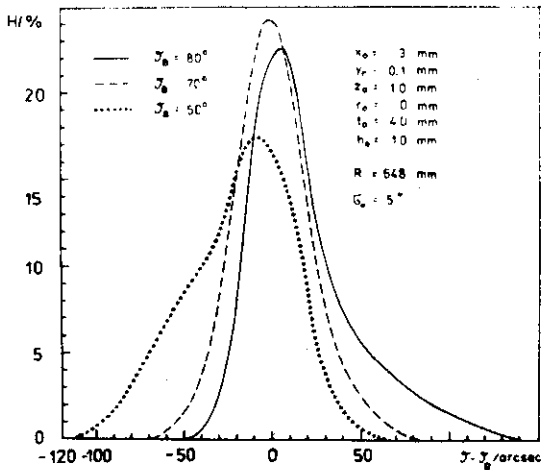
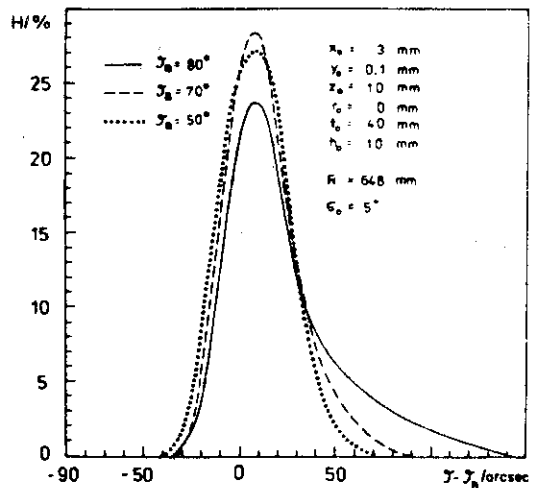


Fig.5. Reflex profile, following after the convolution from Gaussian shaped diffraction pattern (maximum amplitude 1) with the distribution function  $D(\theta_B-\theta)$  for the Bragg case (Johann spectrometer). The reflex amplitude (in percent) is related to the maximum amplitude of the diffraction pattern.

Fig.6. Reflex profile, following after the convolution from Gaussian shaped diffraction pattern (maximum amplitude 1) with the distribution function  $D(\theta_B-\theta)$  for the Bragg case (Johansson spectrometer). The reflex amplitude (in percent) is related to the maximum amplitude of the diffraction pattern.







```

I1B=TB*FLOAT(NH)*TK
SST1B=SIN(T1B)
CCT1B=COS(T1B)
XS=0.
DO 3 J=1,H
XX=X1+XD*%RANF(0.)
Y=Y1+YD*%RANF(1.)
Z=Z1+ZD*%RANF(2.)
R=R1+RD*%RANF(3.)
T=T1+TD*%RANF(4.)
H=H1+HD*%RANF(5.)
XR=XX/PR
YR=Y/RR
RRR=R/RR
TR=T/RR
HZR=(H-7)/RR
RR2=1.+RRR
ST1B=SIN(T1B+TR)
CT1B=COS(T1B+TR)
V=(SST1B-YD)*CT1B-XD*ST1B
W=(SST1B-YD)*ST1B+XD*CT1B
SI=RR2*V/SQRT((RR2-W)**2+V**2+HZR**2)
YS=-(SI-SIN(TB))**2/(SIGM*CCT1B**2)
IF(YS.LT.-2J) YK=J.
IF(YS.LT.-2J) GOTO 4
YK=EXP(YS)
4 CONTINUE
XS=XS+YK
3 CONTINUE
XS=XS/FLOAT(N)
X(I)=XS
2 CONTINUE
GOTO 8
7 CONTINUE
C ***** BRAGG CASE
DO 12 I=1,NS%BK
NH=I-NS%3
I1B=TB*FLOAT(NH)*TK
SST1B=SIN(T1B)
CCT1B=COS(T1B)
XS=J.
DO 13 J=1,H
XX=X1+XD*%RANF(0.)
Y=Y1+YD*%RANF(1.)
Z=Z1+ZD*%RANF(2.)
R=R1+RD*%RANF(3.)
T=T1+TD*%RANF(4.)
H=H1+HD*%RANF(5.)

YR=Y/RR
TR=T/RR
XR=XX/PR
RRR=R/RR
HZR=(H-7)/RR
IF(MTYP2.EQ.2) CTR=COS(CTR)
CT1B=COS(T1B+TR)
ST1B=SIN(T1B+TR)
V=(CCT1B-YD)*ST1B-XR*CT1B
W=(CCT1B-YD)*ST1B+XR*CT1B
RR2=1.+RRR-W
IF(MTYP2.EQ.2) RR2=CTR+RRR-W
SI=RR2/SQRT(RR2**2+V**2+HZR**2)
YS=-(SI-SIN(TB))**2/(SIGM*CCT1B**2)
IF(YS.LT.-2J) YK=J.
IF(YS.LT.-2J) GOTO 14
YK=EXP(YS)
14 CONTINUE
XS=XS+YK
13 CONTINUE
XS=XS/FLOAT(N)
X(I)=XS
12 CONTINUE
8 CONTINUE
YK=TK/ENASMC
11 FORMAT(3X,* I *,I10,5X,* XD *,F23.9)
15 FORMAT(//,1X,*ONE CHANNEL CORRESPONDING TO *,F10.4,2X,*ARCSEC*,//)
RETURN
END

```

```

SUBROUTINE WEIGHT(PI,TB,X1,X0,Y1,Y0,Z1,Z0,R1,R0,T1,T0,H1,H0,PP,N1)
GENERATION OF THE DISTRIBUTION FUNCTION D BY THE MONTE-CARLO METHOD
COMMON/C1/ X(1000),EMASMC,EMASD,SIG1,NTYP1,NTYP2
DO 1 I=1,1000
1 X(I)=0.
Y=0
Z=0
R=PI*EMASD
IF(IN1.LE.3) N1=100000
IF(NTYP1.EQ.1) GOTO 5
C ***** LAUE CASE
2 SIB=SIN(TB)
I=I+1
XX=X1+X0*PANH(0.)
Y=Y1+Y0*PANH(1.)
Z=Z1+Z0*PANH(2.)
R=R1+R0*PANH(3.)
T=T1+T0*PANH(3.)
H=H1+H0*PANH(0.)
XR=XX/RR
YR=Y/RR
RRR=R/RR
TR=T/RR
HZR=(H-Z)/RR
STBTR=SIN(TB-TR)
CTBTR=COS(TB-TR)
V=(SIB-YR)*CTBTR-XR*STBTR
W=(SIB-YR)*STBTR+XR*CTBTR
RR2=1.+RRR

SI=RR2*V/SQRT((RR2-W)**2+V**2+HZR**2)
AT=ASIN(SI)
ATD=(TB-AT)*6.448E+05/EPI
J=IFIX(250.5+ATD)
IF(J.LE.0) J=1
IF(J.GT.1000) J=1000
X(J)=X(J)+1
IF(I.LT.11) GOTO 2
GOTO 6
5 CONTINUE
C ***** 3PAGG CASE
12 COTB=CCS(TB)
I=I+1
XX=X1+X0*PANH(0.)
Y=Y1+Y0*PANH(1.)
Z=Z1+Z0*PANH(2.)
R=R1+R0*PANH(3.)
T=T1+T0*PANH(3.)
H=H1+H0*PANH(3.)
YR=Y/RR
XR=XX/RR
TR=T/RR
RRR=R/RR
HZR=(H-Z)/RR
IF(NTYP2.EQ.2) CTR=COS(TR)
STBTR=SIN(TB+TR)
CTBTR=COS(TB+TR)
V=(COTB-YR)*STBTR-XR*CTBTR
W=(COTB-YR)*CTBTR+XR*STBTR
RR2=1.+RRR-W
IF(NTYP2.EQ.2) PR2=CTR+RRR-W
SI=RR2*V/SQRT((RR2**2+V**2+4Z0**2)
AT=ASIN(SI)
ATD=(TB-AT)*6.448E+05/EPI
J=IFIX(250.5+ATD)
IF(J.LE.0) J=1
IF(J.GT.1000) J=1000
X(J)=X(J)+1
IF(I.LT.N1) GOTO 12
6 CONTINUE
PRINT 7, EMASD
PRINT 4, N1
PRINT 3, X(I),I=1,500)
FORMAT(//,10X,1J(14*),*DISTRIBUTION FUNCTION D(TB-THETA) N= *,
1I10,///)
3 FORMAT(1X,1J(10,2)
7 FORMAT(///,1X,*ONE CHANNEL CORRESPONDS TO *,F10.4,2X,*ARCSEC*//)
RETURN
END

```



5. Zschornack G., Müller G., Musiol G. Geometrical Effects in Curved Crystal Bragg Spectrometers. In: Proc. of the X Int. Symp. on Selected Topics of the Interaction of Fast Neutrons and Heavy Ions with Atomic Nuclei, Gaussig, November 17-21, 1980, GDR.
6. Johann H.H. Z.Phys., 1931, 69, p.185.
7. Johansson T. Z.Phys., 1933, 82, p.507.
8. Piller O., Kern J., Beer W. Nucl.Instr. and Meth., 1973, 107, p.61.

Received by Publishing Department  
on February 5 1981.